Molecular-Dynamics Simulations of Electron-Ion Temperature Relaxation in a Classical Coulomb Plasma

Guy Dimonte and Jerome Daligault
Los Alamos National Laboratory, Los Alamos, New Mexico 87545, USA
(Received 3 June 2008; published 23 September 2008)

Molecular-dynamics simulations are used to investigate temperature relaxation between electrons and ions in a fully ionized, classical Coulomb plasma with minimal assumptions. Recombination is avoided by using like charges. The relaxation rate agrees with theory in the weak coupling limit ($g \equiv$ potential/kinetic energy $\ll 1$), whereas it saturates at $g > 1$ due to correlation effects. The "Coulomb log" is found to be independent of the ion charge (at constant g) and mass ratio >25.

DOI: 10.1103/PhysRevLett.101.135001 PACS numbers: 52.25.Kn, 52.27.Gr

Temperature relaxation between electrons and ions in a thermonuclear plasma is one of many transport processes that must be modeled accurately in order to predict inertial confinement fusion (ICF) [1]. Historically, collisional rates have been uncertain because the long-range Coulomb force leads to logarithmic divergences [2,3]. Moreover, ICF plasmas traverse many physics regimes characterized by collective, quantum, and correlation effects [4,5]. This uncertainty may be why codes that use the Landau-Spitzer rate [2] consistently underestimate the peak ion temperature in ICF experiments [6].

To illustrate the issues quantitatively, consider a weakly coupled, classical plasma. The relaxation of the electron temperature (T_e) toward the ion temperature (T_i) is governed by

$$\frac{dT_e}{dt} = -\nu_{e-i}(T_e - T_i) \tag{1}$$

with a rate of the form

$$\nu_{e-i} = \nu_o \ln\Lambda. \tag{2}$$

Most theories [2–5,7–12] obtain the same prefactor

$$\nu_o = \frac{8}{3} n_i e^4 Z^2 \frac{\sqrt{2\pi m M}}{(m k_B T_i + M k_B T_e)^{3/2}}, \tag{3}$$

where $m(M)$, $e(Ze)$, and n_e (n_i) are the mass, charge, and density of the electrons (ions), and k_B is Boltzman's constant. The difficulty arises in treating the long-range electrical forces, which produces a "Coulomb log" of the form

$$\ln\Lambda = \ln(C\lambda_D/R_c). \tag{4}$$

The electron Debye length $\lambda_D \equiv \sqrt{k_B T_e/4\pi n_e e^2}$ represents the largest impact parameter in a plasma because fields are screened out at larger distances [2,7]. The Landau length $R_c \equiv Ze^2/k_B T_e$ represents the smallest relevant impact parameter because it characterizes the large angle scatterings. The coefficient C was found to be ~1–3, either by estimation [2,7] or various levels of approximation [8–10]. Some models [8,10] found $C \propto 1/\sqrt{1+Z}$ because they used the Debye-Huckel screening length $\lambda_D/\sqrt{1+Z}$. However, more systematic theories are possible for a weakly coupled plasma where

$$g \equiv \frac{Ze^2}{\lambda_D k_B T_e} = \frac{R_c}{\lambda_D} \tag{5}$$

is small because R_C and λ_D are well separated. Kihara and Aono [11] (KA) regularized the divergent integrals for close and distant encounters by introducing a cutoff at intermediate scales which cancels out in the end. Brown, Preston, and Singleton [12] (BPS) removed the singularities by using dimensional continuation to emphasize the short- and long-range effects. KA and BPS both found $C = 0.765$ independent of Z, as is reported in Ref. [13].

Since the variance in C can affect $\ln\Lambda$ during an ICF implosion, there have been attempts to "measure" $\ln\Lambda$ with experiments [14] and molecular-dynamics (MD) simulations [15]. The experiments are conducted by irradiating a solid foil with short-pulse lasers and observing the heat pulse on the backside. However, it is difficult to infer ν_{i-e} accurately since Z and T_e are only estimated and there are significant quantum and correlation effects. MD simulations can calculate ν_{i-e} directly with well-defined plasma conditions and interparticle potentials. However, a Coulomb potential with oppositely charged particles leads to collapse (recombination). This can be avoided with finite (semiclassical) potentials which are also used to model quantum effects in limited regimes. However, such MD simulations are no longer *ab initio* and may test only the semiclassical hypothesis.

Here, we describe MD simulations of temperature relaxation for a purely classical plasma using the actual Coulomb force. These are compared with theory without assuming that semiclassical potentials mimic quantum effects. The simulations employ enough particles to ensure numerical convergence with a statistical uncertainty of ~5%. Recombination is avoided by using positively charged electrons and ions. This does not affect ν_{e-i} since

it depends on Z^2 to leading order, but a neutralizing background is needed. We find excellent agreement with the KA and BPS theories in the weakly coupled regime ($g \ll 1$) where they are valid. We also investigate the moderately coupled regime ($g \sim 1$–20) where ICF implosions begin.

To extract ν_{e-i} from the MD simulations, it is first necessary to solve the relaxation equations with a time-dependent ν_{e-i} since it can vary as $T_e^{-\eta}$ with $0 < \eta < 1.5$. In particular, temperature relaxation is governed by Eq. (1) for T_e and

$$\frac{dT_i}{dt} = \nu_{i-e}(T_e - T_i) \equiv \nu_{i-e}\delta T \tag{6}$$

for the ions, where $\nu_{i-e} = (n_e/n_i)\nu_{e-i} = Z\nu_o \ln\Lambda$ due to charge neutrality $n_e = Zn_i$. The dependence on T_i can be removed by invoking energy conservation $n_eT_e + n_iT_i = n_eT_{eo} + n_iT_{io}$ for $g \ll 1$ since we can ignore the electrostatic energy. This yields

$$T_i = T_{io} - Z(T_e - T_{eo}), \tag{7}$$

where T_{eo} and T_{io} are the initial temperatures. The final equilibration temperature

$$T_\infty = \frac{ZT_{eo} + T_{io}}{Z + 1} \tag{8}$$

is obtained by setting $T_e = T_i = T_\infty$ in Eq. (7). Then, by normalizing time to the initial relaxation rate as $\tau \equiv (Z + 1)\nu_{e-i}(T_{eo})t$ and inserting Eqs. (7) and (8) into Eq. (1), we obtain

$$\frac{dT}{d\tau} = \frac{\varepsilon - T}{T^\eta}, \tag{9}$$

where $T \equiv T_e/T_{eo}$ and

$$\varepsilon \equiv \frac{T_\infty}{T_{eo}} = \frac{Z + T_{io}/T_{eo}}{(1 + Z)}. \tag{10}$$

If ν_{e-i} is constant ($\eta = 0$), Eq. (9) has the familiar solution

$$T_e(t) = T_\infty + (T_{eo} - T_\infty)\exp[-\nu_{e-i}(Z + 1)t]. \tag{11}$$

However, for $g \ll 1$, $\ln\Lambda$ increases with T_e such that $\eta = 1$. Then, the solution is given by

$$(Z + 1)\nu_{e-i}(T_{eo})t = 1 - T + \varepsilon \ln\left(\frac{\varepsilon - 1}{\varepsilon - T}\right). \tag{12}$$

The solution for $\eta = 1.5$ and $Z = 1$ is given by Eq. (8.45) in Ref. [3]. To infer $\nu_{e-i}(T_{eo})$, the MD simulations are fit to these solutions by scaling the time axis.

The MD simulations are performed with the COULMD code in which we solve the classical equations of motion for a specified number of electrons (N_e) and ions (N_i) interacting through the pure Coulomb force. The boundaries are chosen to be periodic. For numerical efficiency, the MD code is based on a parallel implementation of the particle-particle-particle-mesh algorithm [16], which combines high resolution for individual encounters with a rapid, mesh-based, long-range force calculation. Time is normalized to the electron plasma frequency $\omega_{pe} = \sqrt{4\pi n_e e^2/m}$, and the integration time step is varied $\omega_{pe}dt < 0.01$ in order to conserve energy to $<10^{-4}$. Each set of particles is initialized randomly in space and with a Maxwellian velocity distribution at a specified temperature. Each species is first allowed to equilibrate only with itself for a time 0.2–$1/\nu_{e-i}$ during which the energy fluctuations dissipate. The temperature is held fixed by rescaling the particle velocities. Then, the relaxation phase commences for $\nu_{e-i}t \sim 1$–3 by letting the whole system evolve freely.

The simulation parameters are chosen to preserve the physics of interest while mitigating the numerical issues. For a purely classical plasma, the physics issues center on g since Eqs. (2)–(4) reduce to

$$\frac{\nu_{e-i}}{\omega_{pe}} = \frac{1}{3}\sqrt{\frac{8}{\pi}}\frac{m}{M}g\ln\left(\frac{C}{g}\right) \tag{13}$$

for the typical conditions of $m \ll M$ and $T_e \sim T_i$. We can then reduce the run time by reducing the mass ratio to $M/m < 1836$. We typically use $M/m \sim 100$ to preserve the separation of scales between electrons and ions, and we see no statistically significant variation in $\ln\Lambda$ for $M/m > 25$. Since Eq. (3) varies as Z^2, we can use like charges to avoid recombination without affecting ν_{e-i} to leading order. This allows us to avoid making assumptions about interparticle forces by using the actual Coulomb force. However, this does restrict the integration time step to $\omega_{pe}dt < 0.01$ in order to accurately describe the close encounters where the force changes rapidly and the particle deflections are large. As we vary g, we vary the time step and particle number to ensure that the solutions are converged with a statistical variation in $\ln\Lambda$ of $<5\%$. We find that this requires $N_e > 3700/g^{1/3}$ and to $\omega_{pe}dt < 0.02g^{2/3} < 0.01$. The dependence on g occurs because it sets the range of scales that must be resolved to accurately capture all relevant particle interactions. This requires $g \geq 0.006$ since our computer limits us to 10^6 particles and time steps.

To obtain ν_{i-e}, the temporal decay of $T_e - T_i$ from the MD simulations (colored lines) is fit to the analytical solutions (black lines) in Fig. 1 for $g = 0.1$ ($Z = 1$, $M/m = 100$, $n_e = 9 \times 10^{20}$ cm^{-3}, $T_{eo} = 15$ eV, $N_e = 6 \times 10^4$). Figure 1(a) shows the simplest case to analyze because $T_{io} = 12$ eV ($\varepsilon = 0.9 \sim 1$) and the analytical solutions for $\eta \neq 0$ decay with a nearly constant exponential rate $2\nu(T_{eo})t$. Since the natural time unit in the MD simulations is $\omega_{pe}t$, the MD result is fit to the analytical solution by dividing the MD time scale by a scaling factor S. In

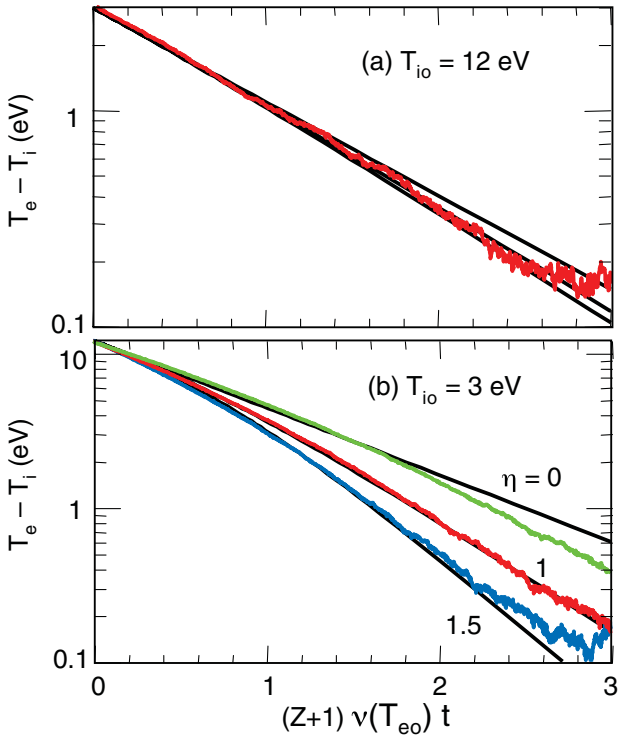

FIG. 1 (color). Temperature difference vs time scaled to initial relaxation rate and ionization for $g = 0.1$ ($Z = 1$, $M/m = 100$, $n_e = 9 \times 10^{20}$ cm^{-3}, $T_{eo} = 15$ eV, $N_e = 6 \times 10^4$). $T_{io} = 12$ and 3 eV in (a) and (b), respectively. Black lines are the analytical solutions for $\eta = 0$, 1, and 1.5 from top to bottom, and the green, red, and blues lines are the respective MD results.

other words, we vary S to obtain the best fit of $T_e(\omega_{pe}t/S) = T_e[2\nu(T_{eo})t]$, and this yields a relaxation rate of $\nu_{\mathrm{MD}}(T_{eo}) = \omega_{pe}/2S$. The MD result (red line) is fit to the analytical solution for $\eta = 1$ (middle black line) with $S = 460$. By using Eqs. (2) and (3) to define

$$\ln\Lambda \equiv \frac{\nu_{\mathrm{MD}}}{\nu_o} = \frac{\omega_{pe}}{2S\nu_o}, \tag{14}$$

we obtain $\ln\Lambda \sim 2.07$. When these data are fit to the analytical solutions for $\eta = 0$ and 1.5 (not shown), we obtain $\ln\Lambda = 2.17$ ($S = 440$) and 2.03 ($S = 470$), respectively. These values are within the 5% statistical uncertainty found for $g = 0.1$ as we varied N_e, M/m, and the equilibration and integration time steps.

The importance of using the solutions with the time-dependent ν_{e-i} to analyze the data is seen in Fig. 1(b) where $T_{io} = 3$ eV ($\varepsilon = 0.6$). Here, the solutions with $\eta \neq 0$ decay more strongly than a simple exponential ($\eta = 0$) because ν_{e-i} increases as T_e decreases from $T_{eo} = 15$ eV to $T_\infty = 9$ eV. The red line shows an excellent fit of the MD result to the solution with $\eta = 1$ (middle black line) using $S = 465$. This corresponds to $\ln\Lambda \sim 2.03$ similar to the result in Fig. 1(a). The same MD data fit to $\eta = 0$ (green line) and 1.5 (blue line) yields poorer correlation coefficients and $\ln\Lambda = 2.51$ ($S = 380$) and 1.78 ($S = 535$), respectively. Thus, we see that the analysis with a simple exponential ($\eta = 0$) yields a value of $\ln\Lambda$ which is systematically large by 22% when $T_{eo}/T_{io} = 5$.

It should be pointed out that the choice of $T_{eo} = T_{io}$ involves numerical compromises and requires an awareness of the solutions. When $T_{eo}/T_{io} \sim 1$, the fractional change in ν_{e-i} is small during the relaxation, but the numerical errors become more important because $T_e - T_i$ is small. Notice that the noise is ~0.2 eV in Fig. 1, and this represents the lower bound in $T_{eo} - T_{io}$. The situation changes for $g > 1$ because we find that ν_{e-i} becomes insensitive to T_e and the simple exponential is the preferred solution for analysis.

The variation of the scaled ν_{e-i} with g is shown in Fig. 2. For $g \ll 1$, the MD results (diamonds) increase with g but not quite linearly (line) because of the dependence of $\ln\Lambda$ on g. These points were analyzed using the analytical solution with $\eta = 1$ as discussed above. For $g > 1$, ν_{e-i} becomes independent of g, which suggests that $\ln\Lambda \propto 1/g$. The results in Fig. 2 were obtained over a wide range of plasma conditions: 5 eV $< T_e <$ 6 keV, 3×10^{18} cm^{-3} $< n_e < 2 \times 10^{26}$ cm^{-3}, $30 < M/m < 1836$, and $10^4 < N_e < 10^6$ depending on g. Simulations with the same g but different T_e and n_e yield the same ν_{e-i}, thereby verifying that g is the dominant parameter for a classical Coulomb plasma.

The MD results can be normalized using Eq. (14) to yield $\ln\Lambda$ as shown in Fig. 3. Within the statistical uncertainty of $\pm 5\%$, the MD results (diamonds) are in excellent agreement with the KA and BPS theories (blue line) for $g < 0.2$ where they are valid. The Spitzer estimate with $C = 3$ (black line) exceeds the MD results by an additive value of $\ln(3/0.765) \sim 1.4$. Of course, these theories ignore correlation effects [4,17] and fail when $g > 0.2$, whereas the MD simulations remain valid. The MD results can be fit to

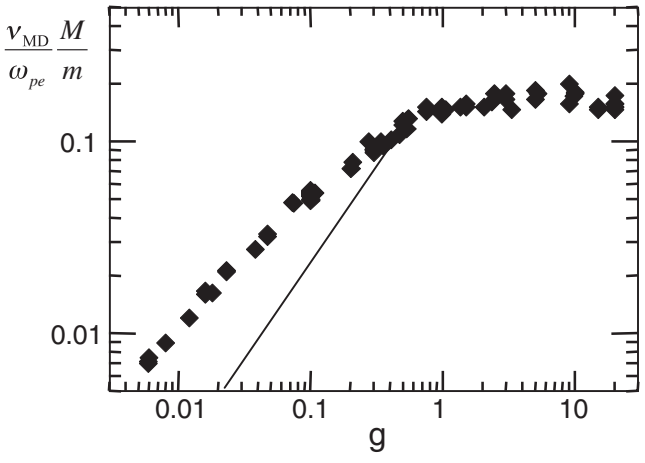

FIG. 2. The scaled temperature relaxation rate from the MD simulations vs plasma parameter g. The line is a visual aid for linear dependence (constant $\ln\Lambda$).

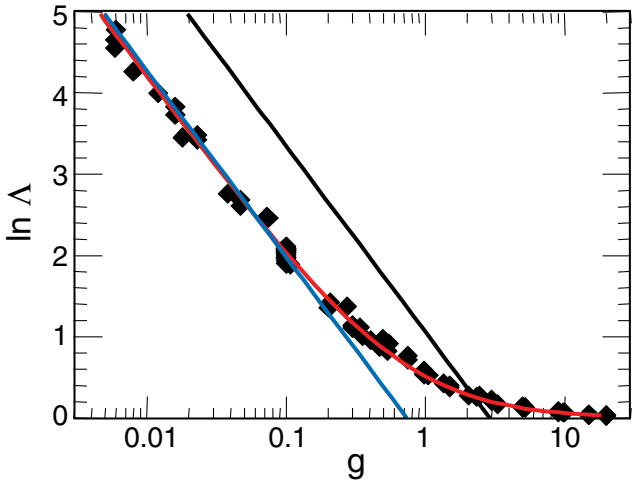

FIG. 3 (color). Coulomb log vs plasma parameter. The diamonds are from MD simulations, while the black line is the Spitzer ($C = 3$) result, the blue line is the KA and BPS theories, and the red line is a numerical fit [Eq. (15)] to the data.

$$\ln\Lambda \sim \ln(1 + 0.7/g) \tag{15}$$

over the entire region, as indicated by the red line. This function is only a numerical fit that reduces to the KA and BPS results for $g \ll 1$ and captures the plateau in ν_{e-i} at large g since $\ln\Lambda \Rightarrow 0.7/g$.

In Fig. 4, the MD simulations (diamonds) show that $\ln\Lambda$ is insensitive to the ion charge at $g = 0.1$. These are conducted with like charges but maintaining "charge neutrality" ($N_e = ZN_i$). The line is normalized at $Z = 1$ but shows the variation $0.5\ln(1 + Z)$ one would expect from Debye-Huckel screening. These results verify that the ions do not participate in the screening during temperature relaxation with electrons since it occurs faster than the ion time scale by $\sqrt{M/m}$. This is consistent with the theories of KA and BPS.

In summary, we have performed MD simulations of electron-ion temperature relaxation for a classical Coulomb plasma without assumptions. For $g < 0.2$, $\ln\Lambda$ agrees with the theories of KA and BPS (where they are valid) to within the statistical uncertainty of $\pm 5\%$ and differ significantly from the commonly used Spitzer estimate. For larger g, $\ln\Lambda \propto 1/g$ due to correlation effects leading to a saturation in ν_{e-i}. In addition, $\ln\Lambda$ is found to be insensitive to Z at constant g, thereby showing that ions do not participate in screening during temperature relaxation. We also see no variation for $M/m > 25$.

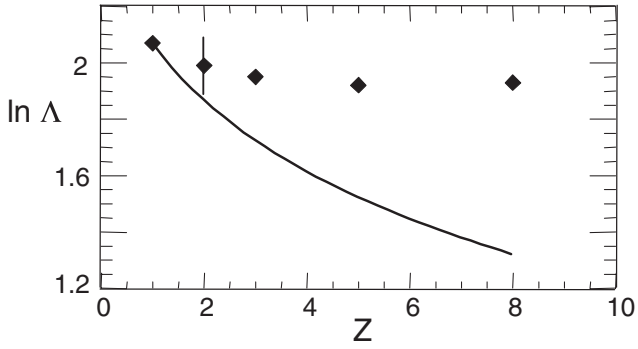

FIG. 4. Coulomb log vs ionization for $g = 0.1$. The diamonds are from MD, and the line is using Debye-Huckel distance $\lambda_D/\sqrt{1 + Z}$.

We thank L. S. Brown, R. Singleton, G. Csanak, and D. Mozyrsky for useful discussions. This work was performed for the U.S. Department of Energy by Los Alamos National Laboratory under Contract No. DE-AC52-06NA2 5396.

[1] S. Atzeni and J. Meyer-Ter-Vehn, *The Physics of Inertial Fusion* (Clarendon Press, Oxford, U.K., 2004).
[2] L. Spitzer, *Physics of Fully Ionized Gases* (John Wiley & Sons, New York, 1962).
[3] D. J. Rose and M. Clark, *Plasmas and Controlled Fusion* (MIT Press, Cambridge, MA, 1961).
[4] S. Ichimaru, *Statistical Plasma Physics Volume I: Basic Principles* (Westview Press, Cambridge, MA, 2004).
[5] Y. T. Lee and R. M. More, Phys. Fluids **27**, 1273 (1984).
[6] D. C. Wilson *et al.*, Phys. Plasmas **11**, 2723 (2004).
[7] L. Landau, Sov. Phys. JETP **7**, 203 (1937).
[8] R. S. Cohen, L. Spitzer, and P. McRoutly, Phys. Rev. **80**, 230 (1950).
[9] W. B. Thompson and J. Hubbard, Rev. Mod. Phys. **32**, 714 (1960).
[10] R. L. Liboff, Phys. Fluids **2**, 40 (1959).
[11] T. Kihara and O. Aono, J. Phys. Soc. Jpn. **18**, 837 (1963).
[12] L. S. Brown, D. L. Preston, and R. L. Singleton (to be published).
[13] E. M. Lifshitz and L. P. Pitaevskii, *Physical Kinetics* (Elsevier, Butterworth and Heinemann, Oxford, U.K., 2006), p. 193.
[14] A. Ng *et al.*, Phys. Rev. E **52**, 4299 (1995).
[15] J. P. Hansen and I. R. McDonald, Phys. Lett. A **97**, 42 (1983).
[16] R. Hockney and J. Eastwood, *Computer Simulations Using Particles* (McGraw-Hill, New York, 1981).
[17] J. Daligault and D. Mozyrsky, Phys. Rev. E **75**, 026402 (2007).